The LINNEAN SOCIETY of London BIOLOGICAL Journal of the Linnean Society

Biological Journal of the Linnean Society, 2012, **107**, 192–209. With 7 figures

Inferring the evolutionary history of divergence despite gene flow in a lizard species, *Scincella lateralis* (Scincidae), composed of cryptic lineages

NATHAN D. JACKSON* and CHRISTOPHER C. AUSTIN

Museum of Natural Science and Department of Biological Sciences, Louisiana State University, Baton Rouge, LA 70803, USA

Received 10 January 2012; revised 24 March 2012; accepted for publication 25 March 2012

Although recent radiations are fruitful for studying the process of speciation, they are difficult to characterize and require the use of multiple loci and analytical methods that account for processes such as gene flow and genetic drift. Using multilocus sequence data, we combine hierarchical cluster analysis, coalescent species tree inference, and isolation-with-migration analysis to investigate evolutionary relationships among cryptic lineages of North American ground skinks. We also estimate the extent that gene flow has accompanied or followed diversification, and also attempt to account for and minimize the influence of gene flow when reconstructing relationships. The data best support seven largely parapatric populations that are broadly concordant with mitochondrial (mt)DNA phylogeography throughout most of the species range, although they fail to fully represent extensive mtDNA divergence along the Gulf Coast. Relationships within and among three broad geographical groups are well supported, despite evidence of gene flow among them. Rejection of an allopatric divergence model partially depends on the inclusion of samples from near parapatric boundaries in the analyses, suggesting that allopatric divergence followed by recent migration may best explain migration rate estimates. Accounting for geographical variation in patterns of gene flow can improve estimates of migration–divergence parameters and minimize the influence of contemporary gene flow on phylogenetic inference. *Biological Journal of the Linnean Society*, 2012, **107**, 192–209.

ADDITIONAL KEYWORDS: coalescence – dispersal – incomplete lineage sorting – migration–divergence – nuclear DNA – phylogenetic inference – Pleistocene – refugia – simulation – south-eastern USA.

INTRODUCTION

How frequently populations diverge and speciate in the face of ongoing gene flow is still an open question in population genetics (Coyne & Orr, 2004). This is in part because a model of parapatric or sympatric divergence accompanied by gene flow is difficult to distinguish from a model of allopatric divergence followed by (post-divergence) gene flow (Coyne & Orr, 2004; Becquet & Przeworski, 2009; Strasburg & Rieseberg, 2011). Determining whether gene flow observed between divergent groups is a recent or long-term phenomenon may not only have implications for understanding the speciation process, but may also impact our ability to reconstruct relationships among these groups. The problems posed by gene flow for species tree inference are well known (Wakeley & Hey, 1998; Nielsen & Wakeley, 2001; Eckert & Carstens, 2008), although they may vary in magnitude and surmountability depending on whether that gene flow is historical or contemporary. For example, if gene flow is a recent phenomenon commencing among divergent populations that have recently come into secondary contact, then focusing analysis on samples collected away from this region of contact may allow us to accurately estimate branching patterns among lineages, despite recent gene flow near their boundaries. However, if gene flow between lineages occurred throughout the divergence process, the

*Corresponding author. Current address: Geomatics and Landscape Ecology Laboratory, Department of Biology, Carleton University, 1125 Colonel By Drive, Ottawa, Ontario, Canada, K1S 5B6. E-mail: nathanjackson@glel.carleton.ca

confounding effects of gene flow and lineage sorting will likely be more difficult to distinguish given that both effects will be geographically pervasive. Given that species tree inference can be misled by recent or ongoing gene flow among groups, when reconstructing relationships near the species level, it is thus important to estimate the extent that gene flow has accompanied or followed divergence and, if possible, to reduce the impact of gene flow's signature on species tree estimation.

In the present study, we investigate the extent that gene flow has accompanied divergence among incompletely sorted lineages of a common North American skink and attempt to estimate evolutionary relationships among these lineages at the same time as accounting for the influence of long-term and recent gene flow. The ground skink, *Scincella lateralis* (Say), is a highly abundant lizard species that is continuously distributed throughout the south-eastern USA, particularly along the Gulf and Atlantic coastal plains (Conant & Collins, 1998). Although no morphological differentiation across populations has been demonstrated (Johnson, 1953), the species displays extensive cryptic genetic diversity and fragmentation across its range (Jackson & Austin, 2010). Mitochondrial (mt)DNA sequences exhibit phylogenetic divergence (up to 8%, uncorrected) among 14 lineages that are distributed parapatrically, although with some overlap near clade boundaries, from central Texas east to the Atlantic Coast (see Supporting information, Fig. S1). A substantial number of these clades are restricted to small, distinct regions along the southern edge of the species range, suggesting a long history of isolation for ground skink populations near the Gulf Coast (Jackson & Austin, 2010). Although multilocus autosomal DNA broadly supports some of the geographically more widely spread mtDNA lineages, it remains unclear whether many of these small divergent mtDNA clades in the south are also reflected in other loci. It is also unclear what role dispersal has played in *S. lateralis* diversification. Have populations diverged largely in isolation, followed by relaxation of dispersal barriers since the Pleistocene, or has diversification taken place in the face of long-term dispersal that has continuously or intermittently (with fluctuating climate cycles) occurred among populations?

Additionally, although relationships among lineages inferred using mtDNA are well-supported, relying upon the history of a single gene to infer the history of a species can lead to erroneous conclusions (Pluzhnikov & Donnelly, 1996; Maddison, 1997; Kuo & Avise, 2005). Several stochastic and deterministic forces may affect the mitochondrial genome, which have nothing to do with the history of isolation and dispersal being inferred (Hudson & Coyne, 2002; Zink, 2005). However, inferring evolutionary relationships among groups using multilocus data is fraught with its own set of challenges (Edwards, 2009), particularly when those groups are recently divergent, morphologically cryptic, and potentially exchanging dispersers, as is the case for *S. lateralis*.

In the present study, we investigate the history of isolation and dispersal in *S. lateralis* using multilocus sequence data. Our approach is first to estimate the number and geographical distribution of distinct populations by using hierarchical cluster analysis. Accordingly, we have expanded the multilocus sampling of a previous study (Jackson & Austin, 2010) to more intensively represent populations near the Gulf Coast where the highest diversity has been observed. Second, we reconstruct evolutionary relationships among these inferred groups using coalescent species tree analysis implemented using the software *BEAST. Third, we test whether divergence among groups better fits an allopatric or isolation-with-migration model and attempt to account for and minimize the effects of gene flow on species tree inference. Specifically, we address three questions in regards to the impact of gene flow among groups: (1) to what extent does gene flow occur between inferred populations; (2) has gene flow been largely historical (i.e. accompanying divergence that took place in sympatry or parapatry) or recent (i.e. post-dating divergence that took place in allopatry); and (3) how robust is species tree inference to the effects of gene flow?

MATERIAL AND METHODS

Sampling

We used 142 samples from 75 sites across the range of *S. lateralis* (Fig. 1; see also Supporting information, Table S1). Sampling was designed to represent geographical range and to adequately test divergence hypotheses based on previously observed patterns of genetic variation in the group (Jackson & Austin, 2010). For the present study, sequence data from eight nuclear loci (4673 total base pairs; see Supporting information, Table S2) were collected from 80 of these samples and combined with data for the remaining 62 samples that had been used previously (Jackson & Austin, 2010). These loci include one intron: selenoprotein T (SELT; 852 bp); one protein-coding gene: the prolactin receptor (PRLR; 558 bp); and six noncoding genomic loci (ranging from 443 to 641 bp). *Scincella gemmingeri* was included as an outgroup.

Generation of genetic data

Liver or tail tissue was sampled from each lizard and preserved in $\geq$ 95% ethanol and/or stored at –80 °C.

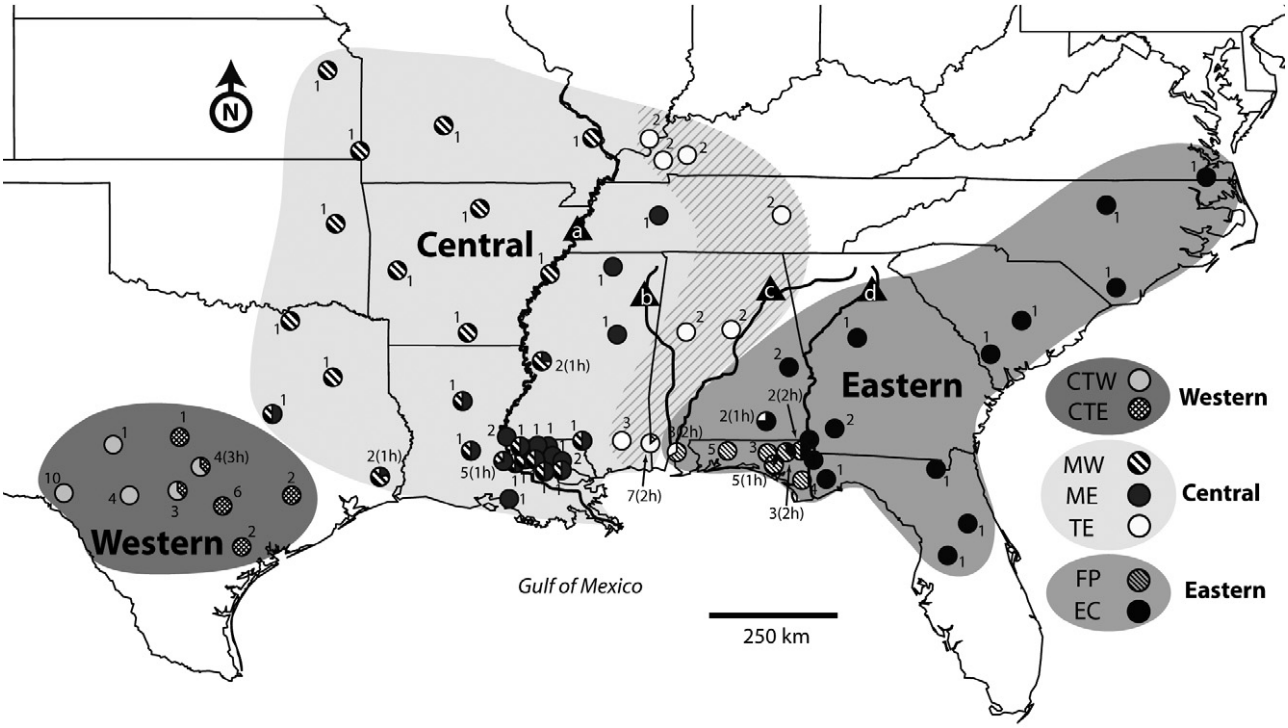

Figure 1. Geographical distribution of populations inferred using STRUCTURE. The number of samples per site is indicated for each locality, with the number of hybrids (those assigned with > 0.30 probability to both populations) in parenthesis. Circle shading is proportional to the total probability of population assignment per site. CTE, central Texas west; CTW, central Texas east; EC, East Coast; FP, Florida Panhandle; TE, east of the Tombigbee River; ME, Mississippi River east; MW, Mississippi River west. Shading corresponds to three major lineages inferred using species tree analysis. These groups also correspond with three upper-hierarchy STRUCTURE clusters, except in the case of the STRUCTURE results, population TE (identified by diagonal lines) is in the eastern group. Four phylogeographically important rivers are labeled with letters: (a) Mississippi, (b) Tombigbee, (c) Alabama, and (d) Apalachicola.

Genomic DNA was extracted from liver tissue using salt-extraction (Fetzner, 1999) and from tail tissue using a Qiagen DNeasy extraction kit (Qiagen). A polymerase chain reaction and amplicon purification were carried out in accordance with standard protocols (Austin *et al*., 2010) and double-stranded cycle-sequencing was carried out using the BigDye Terminator cycle-sequencing kit, version 3.1 (Applied Biosystems). After sequences were cleaned using Sephadex, they were electrophoresed on a 3100 Genetic Analyzer (Applied Biosystems).

Sequences were edited and assembled into contigs using SEQUENCHER, version 4.6 (GeneCodes) and the PRLR dataset was translated into amino acids to check alignment. The alignment of noncoding regions was carried out using CLUSTAL X, version 2.0 (Larkin *et al*., 2007) and the results were adjusted by eye. Haplotype phase was inferred computationally using PHASE, version 2.1 (Stephens, Smith & Donnelly, 2001; Stephens & Scheet, 2005). We tested for intra-locus recombination by scanning each alignment for violations of the four-gamete rule (Hudson & Kaplan, 1985) using the software IMGC (Woerner, Cox & Hammer, 2007). Using this method, we then constructed a recombination-free alignment by removing a combination of recombining sites and samples in a way that maximizes the data available for use in subsequent analyses.

Hierarchical population genetic structure

We first investigated hierarchical population structure using the clustering method implemented in STRUCTURE, version 2.2.3 (Pritchard, Stephens & Donnelly, 2000). This method estimates the likelihood of the data under a fixed number of populations (K) and the most probable assignment of individuals to populations, given this K-value. When comparing likelihoods under a range of K-values, the modal value of ΔK (a statistic relating to the rate of change in the log likelihood of the data across a continuous series of K) reliably corresponds to the K-value representing the highest level of population structure within a dataset (Evanno, Regnaut & Goudet, 2005).

Once this upper-level structure has been inferred, population sub-structure within a set of populations (inferred upon initial analysis) can be investigated by repeating cluster analysis on each population separately.

We applied the linkage model (Falush, Stephens & Pritchard, 2003) to the phased sequence data that allows admixture among populations and linkage within but not among the eight loci. We ran STRUCTURE, for all values of K between $K = 1$ and $K = 14$, ten times each for 150 000 generations (with an additional burn-in of 150 000). Once the optimal K-value was ascertained by calculating ΔK using the STRUCTURE HARVESTER, version 0.56.4 (http://taylor0.biology.ucla.edu/struct_harvest/), we repeated the STRUCTURE analysis on each of the inferred populations separately (for all values of K between $K = 1$ and $K = 10$). This process was repeated until no additional structure was detectable.

To investigate the possibility that the genetic structure inferred above is an artefact of isolation by distance, we next tested for a relationship between genetic and geographical distance within each inferred population. We first computed pairwise patristic distances among alleles for each locus and population. From these, we calculated a single standardized multilocus pairwise distance matrix among individuals for each population using POFAD, version 1.03 (Joly & Bruneau, 2006). The statistical correlation between genetic distance matrices and pairwise great circle geographical distances was evaluated using Mantel tests (implemented with IBD, version 1.52, for 10 000 permutations; Bohonak, 2002).

Species tree inference

To infer relationships among populations, we used a method of species tree inference implemented in the program *BEAST, version 1.5.3 (Heled & Drummond, 2010). This method infers a population tree at the same time as modeling the coalescent process that gave rise to it. First, we carried out species tree analysis using the full multilocus dataset, where the seven populations inferred using STRUCTURE (Figs 1, 2) were defined as 'species'.

Second, to explore the robustness of inferred relationships to varying levels of intra-population sampling, we next iteratively sub-sampled the full dataset for four different sample sizes (two, four, eight, and sixteen gene copies). For each sampling regime, we generated 100 datasets by randomly sampling from the original dataset without replacement and then performed species tree analysis on each replicate. We then summarized the posterior distribution of species trees across all replicates (within a sampling regime) by constructing 50% consensus trees from post-burn-in samples. Posterior probabilities (*PP*) at nodes in this case represent the average support for each node across independent replicates. High values indicate that a node is well supported under a particular sample size.

Finally, we tested whether the inferred species tree topology was significantly more likely than two alternative topologies based on observed patterns of genetic divergence or mtDNA phylogeny. First, both traditional phylogenetic analysis (results not shown) and hierarchical structure analysis indicate that the inferred western group (containing two populations: 'central Texas west' or CTW and 'central Texas east' or CTE; Figs 1, 2) is the most distinct group within *S. lateralis*. This is in contrast to the estimated species tree, which infers the eastern group to be the most basal (Fig. 3). Second, mtDNA phylogeny places CTE samples (approximately corresponding to mtDNA clade c; see Supporting information, Fig. S1) into the central group, whereas, species tree inference based on multilocus data nests CTE samples with CTW samples within the western group. To test whether the most likely species tree topology is significantly more likely than these two alternative topologies, we performed separate species tree analyses where topologies were constrained based on these two alternative hypotheses: *Constraint 1*: the two central Texas populations (CTW and CTE) are basal to all other populations and *Constraint 2*: population CTE is nested within the central group. We then used Bayes factors (Kass & Raftery, 1995; Nylander *et al*., 2004) to compare the relative fit of the constrained and unconstrained models. Given large errors associated with estimating Bayes factors (Suchard, Weiss & Sinsheimer, 2005; Beerli & Palczewski, 2010), we took a conservative approach to their calculation. We performed ten independent *BEAST runs under each unconstrained and constrained model. Then, rather than comparing the harmonic mean of the marginal likelihood distributions resulting from the competing hypotheses, we computed quasi-Bayes factors by comparing the lowest post-burn-in log likelihood resulting from all ten unconstrained analyses with the highest post-burn-in log likelihood from the ten constrained analyses. A quasi-Bayes factor of $2\log(BF_{10}) > 10$ was considered strong support for the optimal unconstrained tree (Kass & Raftery, 1995).

For all *BEAST analyses, potential hybrid individuals and portions of sequences that have undergone recombination were removed from the dataset. Hybrid individuals were defined as those samples assigned to two different populations with > 0.30 probability in STRUCTURE. We chose 0.30 as the cut-off for hybrids because this was the approximate threshold above which a positive correlation between dual-ancestry and proximity to a neighbouring popu-

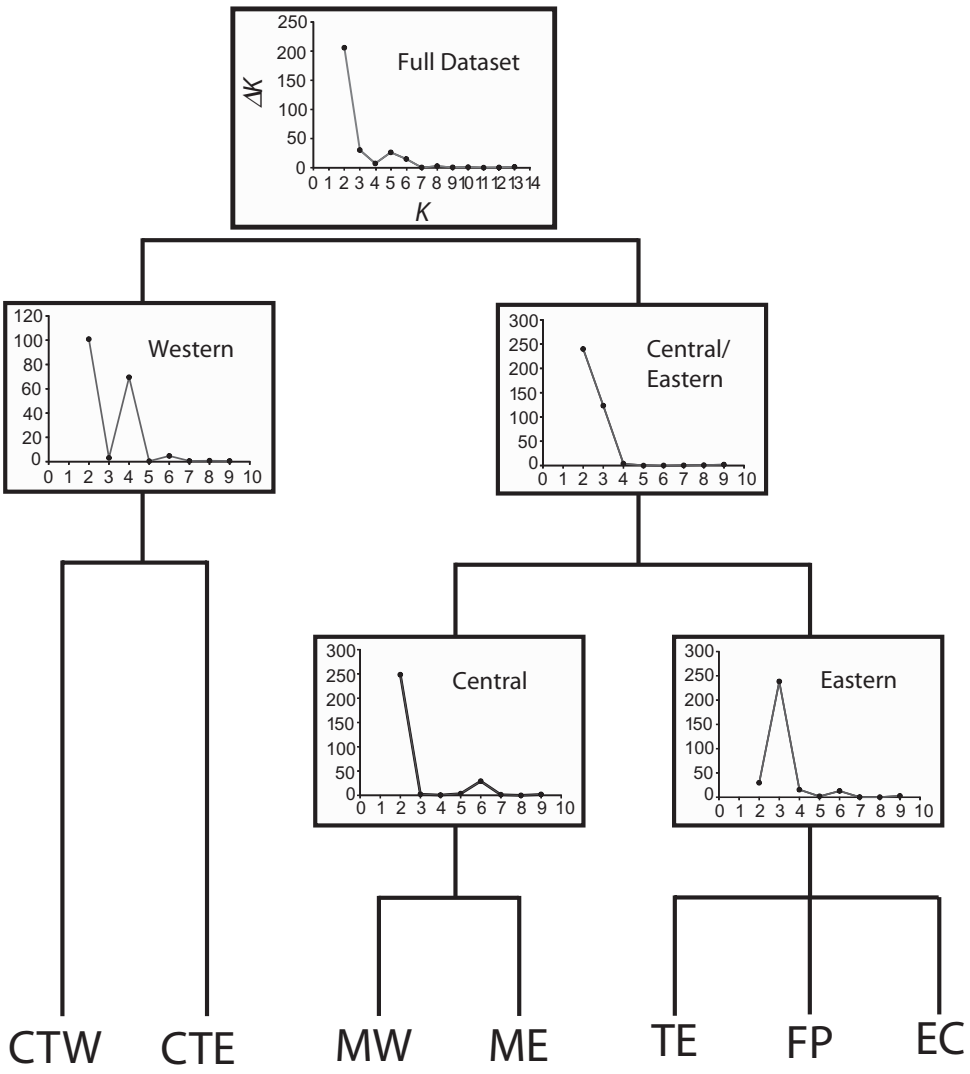

Figure 2. Values of ΔK calculated across hierarchically nested STRUCTURE analyses performed assuming varying numbers of K populations. ΔK peaked at $K = 2$ clusters in all analyses, except analysis of the eastern group where ΔK peaked at $K = 3$. The analysis resulted in three levels of hierarchical structure and seven populations (which correspond to those whose distribution is mapped in Fig. 1). CTE, central Texas west; CTW, central Texas east; EC, East Coast; FP, Florida Panhandle; TE, east of the Tombigbee River; ME, Mississippi River east; MW, Mississippi River west.

lation was apparent. A Jeffreys prior was used for population growth (although more informative priors based on estimates of θ from isolation-with-migration analysis were also tried), a Yule process was assigned to the species tree prior, and substitution, clock, and tree models were unlinked among loci. Best-fit substitution models were applied as inferred using Bayesian information criterion implemented in TOPALI, version 2.5 (Milne *et al*., 2009). To facilitate an approximate calibration for divergence time estimation, we first calculated the divergence time between *S. lateralis* and *S. gemmingeri* assuming a cytochrome b (cyt *b*) evolution rate of 1–2% per million years, which is a range commonly observed in small-bodied lizards (Austin, 1995; Brown & Pestano, 1998; e.g., Malhotra & Thorpe, 2000; Poulakakis *et al*., 2005). We then used these divergence times as a calibration point to estimate a range of rates for each nuclear locus. For the species tree analysis, we applied a uniform distribution to the estimated prior rate of one locus (SELT; 1.106×10^{-9} to 2.212×10^{-9} substitutions/site year^{-1}). We allowed all rates to vary according to an uncorrelated lognormal-distributed relaxed molecular clock. All Markov chains were run for 100 million generations with parameter sampling commencing at generation 10 million (to allow for burn-in) and occurring every 10 000 steps thereafter. Adequate parameter convergence and chain mixing

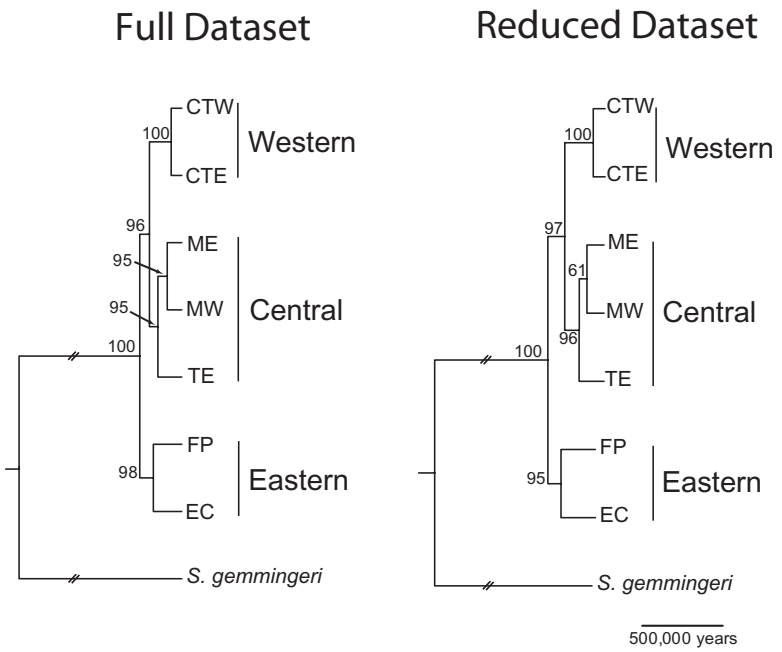

Figure 3. Consensus population trees inferred using species tree analysis implemented in *BEAST under the assumption of seven STRUCTURE populations. Results are shown for analyses involving both full and reduced datasets. The reduced dataset was culled by removing samples nearest the boundaries between parapatric populations. Posterior probability of each node is indicated as a percentage and double-hatched markings indicate branch lengths that have been shortened. CTE, central Texas west; CTW, central Texas east; EC, East Coast; FP, Florida Panhandle; TE, east of the Tombigbee River; ME, Mississippi River east; MW, Mississippi River west.

were assessed for each analysis by comparing estimates across multiple independent runs and evaluating evolutionarily stable strategy values of parameters using TRACER, version 1.5 (Drummond & Rambaut, 2007). We constructed consensus trees from post-burn-in trees that we pooled from five independent runs.

Isolation with migration

The species tree model does not account for gene flow between populations. Thus, to assess the extent that gene flow has occurred between populations, we fit two nested divergence models to the data using IMA2 (Hey, 2010). First, for select population comparisons, we fit a full isolation with migration (IM) model that includes bi-directional migration rate (m), effective population size scaled by mutation (θ), and divergence time (t) parameters. Second, we fit a strict allopatric model that differs from the IM model only in that migration rates were set to zero. We then compared the relative fit of these two models using log-likelihood ratio (LLR) tests. We were unable to include all populations inferred using STRUCTURE (seven total) in a single IM analysis as a result of the modest number of loci in our dataset. Thus, we fit divergence models to all population pairs that: (1) show evidence for a sister relationship (in STRUCTURE or phylogenetic analysis) and/or (2) are geographically adjacent (for a total of eight comparisons).

The effects of IM on parameter estimates are difficult to distinguish from the effects of allopatric isolation followed by recent migration upon secondary contact (Coyne & Orr, 2004; Becquet & Przeworski, 2009; Strasburg & Rieseberg, 2011). We attempted to determine the relative plausibility of these hypotheses by repeating the IM analyses described above using a dataset from which we removed samples nearest the boundaries between neighbouring populations. If gene flow played an important role in the divergence process, its signal should be evident even when only samples far from the current region of parapatry or overlap are considered. However, gene flow detectable only near contemporary population boundaries is regarded as more likely being the result of recent migration between populations that previously diverged in allopatry. For this analysis, we retained only the 16–20 most geographically interior samples for each population in the dataset.

All IM analyses were performed using datasets from which four-gamete rule violations were removed. Because the IM model assumes random sampling from within populations, we included no more than three individuals from a site (selected at random),

although, for analyses where sample size was limited, some excluded samples were reincorporated. Additionally, to avoid the effects of current interbreeding on parameter estimates, STRUCTURE-inferred potential hybrids were excluded from all analyses (based on the > 0.3 probability threshold). Once optimal priors and heating schemes were devised upon initial exploration, 20 independent Markov chains and two independent runs (adjusting only the starting seed) were performed for each analysis. At least 50 000 genealogies were saved per run after a sufficient burn-in period was implemented and all trend plots and posterior parameter densities were visually inspected and compared across runs to confirm adequate Markov chain Monte Carlo (MCMC) mixing and convergence. For conversion of divergence time estimates to an approximation in years, we assumed a generation time of 1.7 years (Jackson & Austin, 2010) and a mean mutation rate of 1.577×10^{-9} substitutions/site year^{-1} [mean per locus rate adjusted for generation time and mean locus size (584.5 bp) is 1.567×10^{-6} substitutions/locus/generation] based on a 1.5% cyt *b*-based calibration (using the method described in the previous section). For LLR tests comparing full (IM) and reduced (allopatric) models, at least 100 000 sampled trees pooled from independent MCMC runs were used to calculate LLR test statistics and a chi-squared test was carried out to assess significance.

Accounting for gene flow in species tree inference

In attempt to account for and minimize the influence of gene flow on species tree inference, we first reduced the impact of currently ongoing gene flow on tree reconstruction by repeating the *BEAST analysis where samples most likely affected by contemporary introgression (near regions of parapatry or overlap) were removed from the dataset (as explained above).

We next investigated the possibility that species tree estimation has been misled by gene flow that remains significant (relative to the allopatric model) even when only the most geographically interior samples are analyzed. After parapatric samples were removed from the dataset, the population found approximately east of the Tombigbee River in Alabama (population TE; Fig. 1) appears to exchange migrants with the two central populations surrounding the Mississippi River (Mississippi River west and east, MW and ME). Thus, the sister relationship inferred between TE and the central group using *BEAST (Fig. 3) could be an artefact of gene flow rather than the result of these groups sharing a most recent common ancestor. One plausible scenario is that population TE could have most recently diverged from the eastern group [composed of populations Florida Panhandle (FP) and the East Coast (EC)] and subsequently engaged in limited gene flow upon secondary contact with the central group (a history depicted in Fig. 4B), causing *BEAST to be misled. A closer relationship between TE and the eastern populations might be predicted a priori given the historical importance of the Tombigbee River in isolating populations of a wide-range of taxa (Soltis *et al*., 2006).

To investigate whether such a scenario could lead to incorrect species tree inference, we generated sequence datasets using coalescent simulations for the three relevant groups (Central, Eastern, and population TE) under this alternative topology (Central,(TE, Eastern)). The simulation was performed twice: first, assuming no gene flow after splitting events (Fig. 4A) and second, assuming that gene flow commenced between Central and TE once TE split from Eastern (Fig. 4B). Both histories were simulated 100 times using SIMDIV (http://genfaculty.rutgers.edu/hey/software) under empirical estimates of migration, θ, and divergence time obtained using IM analysis (see Supporting information, Fig. S2). Given that the chronology of divergence times estimated using IM does not correspond to this simulated history, we assumed: (1) the splitting time between Eastern and TE equals the IM estimate for the Central–TE split and (2) the splitting time between the Eastern/TE group and the Central group equals the IM estimate for the splitting time between Central/TE and Eastern groups. Number and length of loci, sample size, and transition/transversion ratio matched those of the empirical dataset. After species tree analyses were completed, 50% consensus trees were constructed for each scenario using the post-burn-in posterior distribution of trees.

To test whether the inferred species tree relationship (Eastern,(TE, Central)) is significantly more likely than the alternative (Central,(TE, Eastern)), we performed one additional constraint test, where the alternative relationship was forced in a separate *BEAST analysis and quasi-Bayes factors were used to compare the relative fit of the constrained and unconstrainaed models.

Finally, we investigated whether application of an IM model could help resolve the ambiguous placement of TE given the assumption that divergence time will be smallest and gene flow will be highest between sister populations. To assess how migration and divergence time estimates differ under the two hypotheses, we performed two pairwise IM analyses: (1) one including Central and TE and (2) the other including Eastern and TE. Genetic structure within populations (as exists within the central and eastern groups) does not appear to significantly affect IM

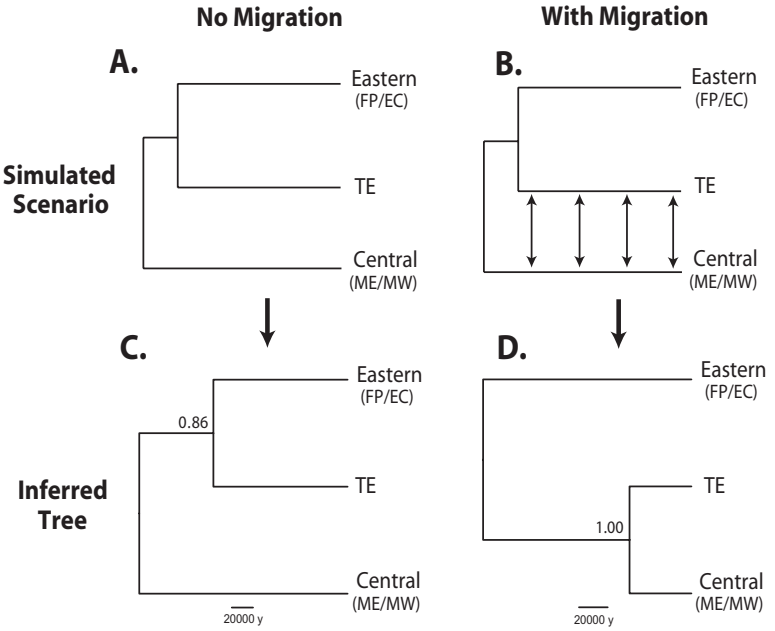

Figure 4. Evolutionary history among eastern, central, and TE (east of the Tombigbee River) populations simulated using SIMDIV without (A) and with (B) post-divergence gene flow, and evolutionary history reconstructed from these simulated datasets using species tree analysis (C, D). Posterior probabilities are from across all simulated replicates. EC, East Coast; FP, Florida Panhandle; TE, east of the Tombigbee River; ME, Mississippi River east; MW, Mississippi River west.

estimates of migration and divergence (Strasburg & Rieseberg, 2010).

RESULTS

Generation of genetic data

Haplotype phase was reconstructed with a *PP* of 1.0 for 96% of samples and with a probability > 0.6 for 98.7% of samples. A few samples (five for PRLR and ten for SELT) were reconstructed with a $PP < 0.60$ and thus were removed from further analysis (Harrigan, Mazza & Sorenson, 2008). Nine sequences were unreadable as a result of heterozygous indels and were also removed from the dataset. Violations of the four-gamete rule were detected to some extent in all loci. The resulting filtered dataset retained an average of 92% of haplotypes for each locus and only two loci, P2-03 and P2-42, were truncated (to 94% and 71% of their original length, respectively). Diversity indices are reported for each locus in the Supporting information (Table S3).

Hierarchical population genetic structure

STRUCTURE analysis using the ΔK method resulted in three hierarchical levels of population structure and seven populations (Figs 1–2). For the overall dataset, ΔK peaked at $K = 2$ with central Texas samples (the 'Western' group) separated from everything else. Subsequent analysis of western samples produced a ΔK peak at $K = 2$ separating 'central Texas east' samples (CTE) from 'central Texas west' samples (CTW). Analysis of the remaining samples (i.e. those not in group Western) yielded a ΔK peak at $K = 2$ separating samples approximately east of the Alabama–Mississippi border (the 'Eastern' group) from everything else (the 'Central' group). Further sub-structuring was detected for group Central (ΔK peak at $K = 2$) with samples approximately separated east (ME) and west (MW) of the Mississippi River, although with extensive geographical overlap. Finally, ΔK from analysis of group Eastern peaked at $K = 3$ and populations were assigned to three geographical regions: (1) approximate to or east of the Tombigbee River (TE); (2) the FP; and (3) the EC. Further analysis of these seven populations where $K > 1$ resulted in purely admixed groups without improvement in log-likelihoods. Mixed ancestry (as defined by the > 0.3 probability threshold) was inferred from several samples that were almost always observed near bordering populations (Fig. 1), justifying our treatment of these samples as hybrids rather than repositories of incompletely sorted alleles.

No significant correlation between genetic and geographical distance was detected for any population after a Bonferroni correction, suggesting that inferred phylogeographical fragmentation in the multilocus

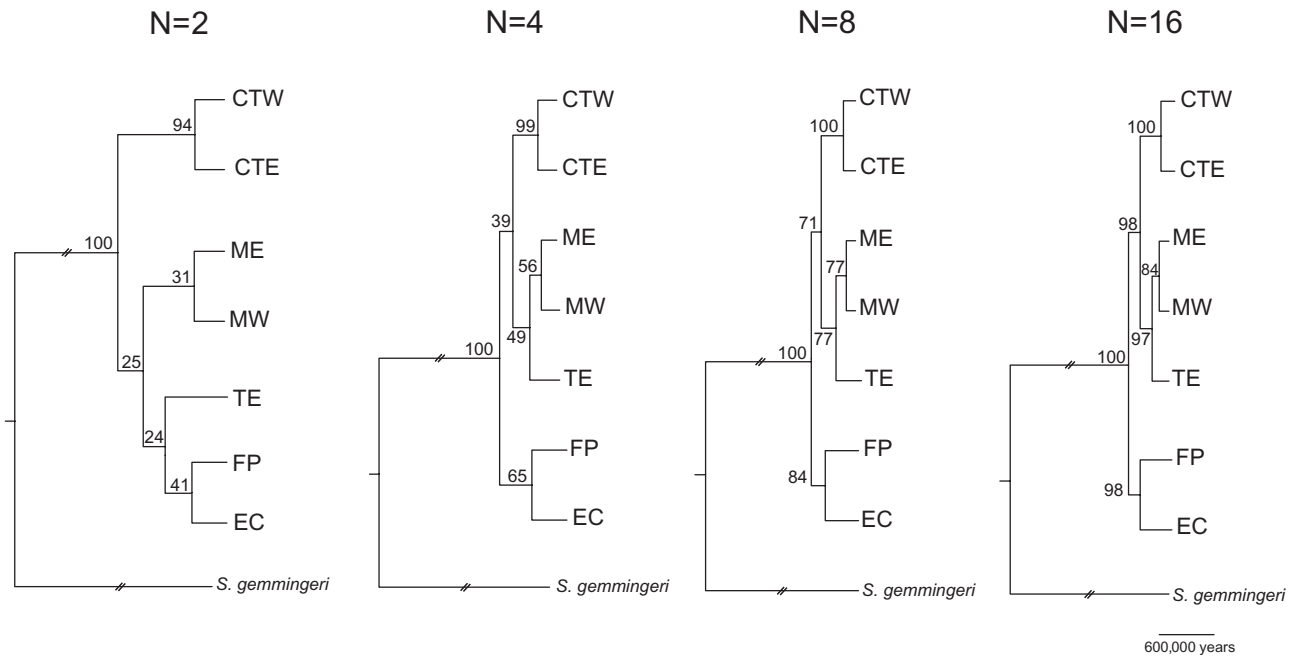

Figure 5. Consensus population trees inferred using species tree analysis under four sampling schemes whereby 100 datasets were randomly generated for each (with two, four, eight, and 16 gene copies per population) from the full dataset. Bipartition frequencies are given at each node and indicate the frequency of all replicates supporting a relationship. CTE, central Texas west; CTW, central Texas east; EC, East Coast; FP, Florida Panhandle; TE, east of the Tombigbee River; ME, Mississippi River east; MW, Mississippi River west.

data is not an artefact of isolation by distance (see Supporting information, Table S4).

Species tree inference

The inferred species tree exhibited high support for relationships among the seven populations (plus outgroup species), consistent across independent searches (Fig. 3). 'Western', 'Central', and 'Eastern' groups were inferred. These groups are the same as those inferred using hierarchical structure analysis, except that population TE is nested within the central group using *BEAST instead of the eastern group. When the full dataset was sub-sampled across four different sample sizes, the western group was consistently supported, regardless of the number of gene copies analyzed. For the remaining nodes, up to 16 gene copies (or more) were required before being inferred in a high proportion of replicates (i.e. 95%; Fig. 5). Marginal log-likelihoods were significantly higher for an unconstrained species tree relative to the two constrained trees, rejecting the STRUCTURE and mtDNA-inferred hypotheses (Table 1).

Table 1. Log-likelihoods and quasi-Bayes factors for comparisons between unconstrained (H_0) and constrained (H_1) phylogenetic models implemented in *BEAST

Constraint	Lower log (H_0)	Upper log (H_1)	2 log (B_{10})
Western is basal	–9475	–9660	370
CTE is nested within Central	–9475	–9767	584
TE is nested within Eastern	–9475	–9758	566

ISOLATION WITH MIGRATION

For the full dataset, divergence in isolation was rejected in five out of the eight pairwise analyses (see Supporting information, Table S5), suggesting that migration has played a role in the divergence process. When parapatric samples were removed from the dataset, allopatric divergence was rejected in only two of the eight analyses (see Supporting information, Table S5), demonstrating the influence of sampling on migration rate estimates. These analyses generally yield increased estimates of divergence time (t averages 0.13 higher, $P = 0.032$, paired t-test) and decreased estimates of migration rate (m averages 0.27 higher, $P = 0.016$, paired t-test) relative to the full datasets (Fig. 6) as is expected if introgressed individuals have been preferentially removed. Estimates of θ do not differ consistently between full and reduced datasets.

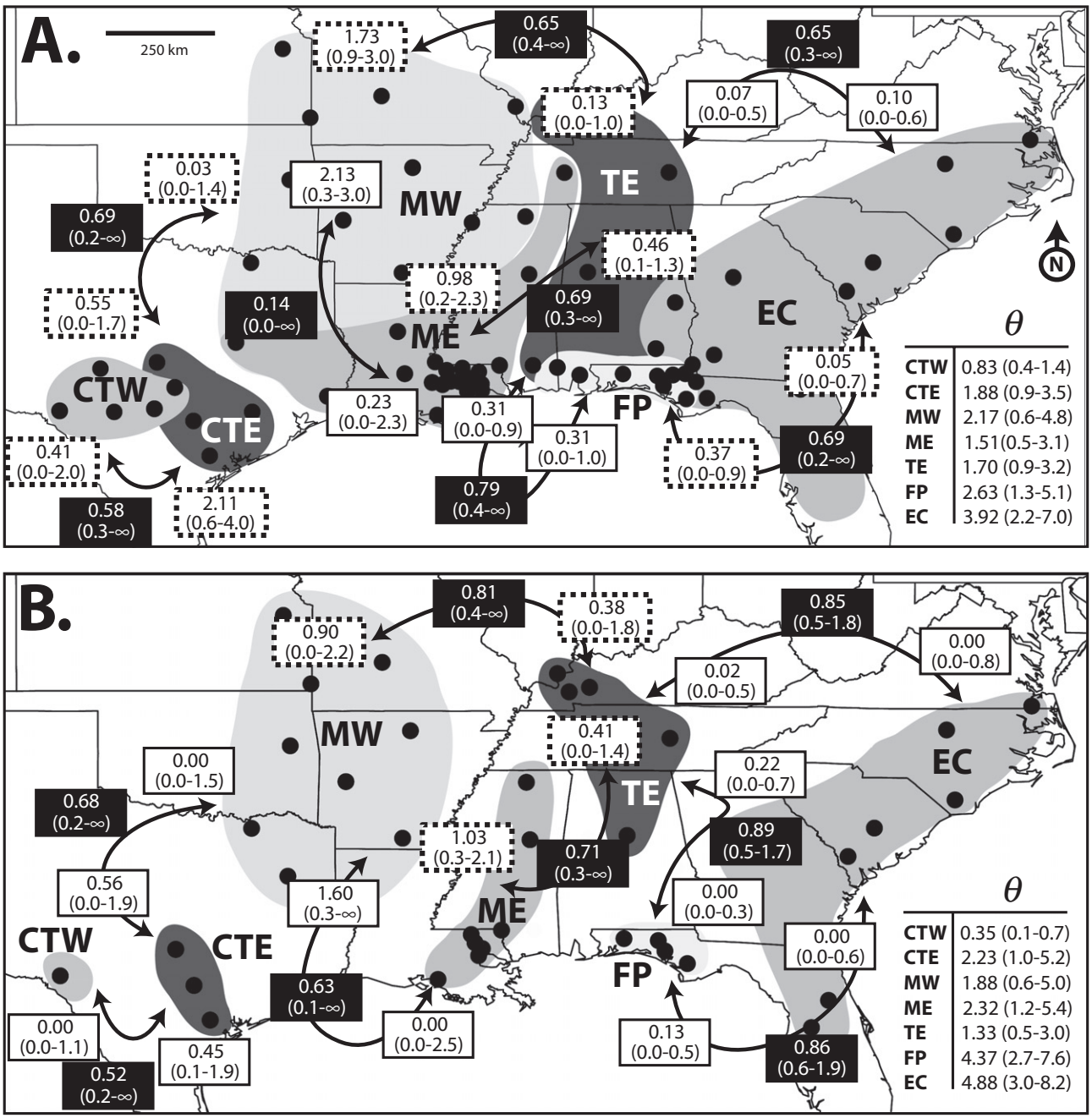

Figure 6. Most likely estimates and 90% highest posterior density (HPD) intervals for demographic parameters from pairwise isolation with migration analyses involving seven *S. lateralis* populations. Analyses were run for full (A) and reduced (B) datasets (wherein samples near parapatric boundaries were removed). Each arrow between any two populations is accompanied by two white squares (which contain migration rates, m) and one black square (which contains divergence time, t). Migration is in the direction indicated by the closest arrowhead. Estimates of θ ($= 4N_e\mu$) given are averaged across all analyses involving a particular population, and 90% HPD intervals (in parentheses) include the lowest and highest values from among these analyses. All parameters are scaled by the neutral mutation rate. HPDs that include ∞ indicate analyses that failed to converge to zero. Migration rates from population comparisons for which the strict isolation model was rejected in log-likelihood ratio tests of nested models are highlighted by a dashed border. CTE, central Texas west; CTW, central Texas east; EC, East Coast; FP, Florida Panhandle; TE, east of the Tombigbee River; ME, Mississippi River east; MW, Mississippi River west.

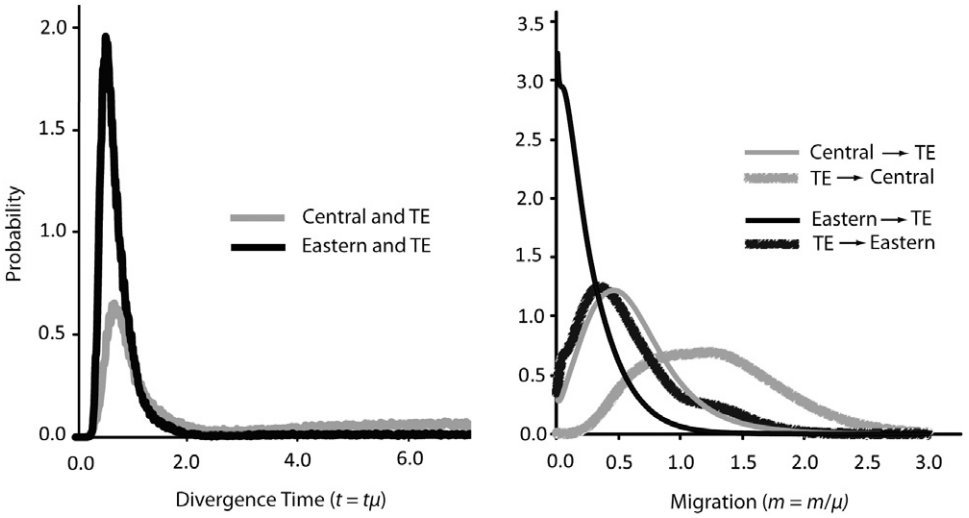

Figure 7. Posterior probability estimates for divergence time and migration rate parameters from isolation with migration analysis of populations (1) Central (Mississippi River west and east) and TE (east of the Tombigbee River) and (2) Eastern (Florida Panhandle and the East Coast) and TE.

Estimates of time since divergence among these populations range from approximately 90 000 years (between ME and MW) and 505 000 years (between TE and FP) before present when the cyt *b*-calibrated evolutionary rate is assumed. Effective population size estimates tend to increase from west to east, with the highest diversity inferred on the east coast (Fig. 6). Migration tends to be asymmetrical, with the highest rates of migration usually moving from eastern to western populations (with the exception of CTW↔CTE, where migration is highest eastward).

Accounting for gene flow in species tree inference

First, when species tree analysis was repeated upon removal of parapatric samples from the dataset, the same topology was inferred as with the full dataset, although the *PP* of the (ME,MW)TE relationship was reduced (Fig. 3). Second, species tree analysis of replicate datasets simulated under the alternative history (Central(TE, Eastern)) without gene flow led to inference of the simulated relationship in a majority of replicates (*PP* of node 1 equals 0.86; Fig. 4C). However, when empirically derived levels of gene flow were incorporated into the simulation, relationships supported by the original species tree analysis were inferred (*PP* of node 1 equals 1.00; Fig. 4D), indicating that gene flow has misled inference of branching patterns. Third, the unconstrained species tree yielded significantly higher marginal log-likelihoods than a tree where population TE was constrained to diverge from the Eastern group (Table 1). Finally, IM estimates of divergence time are similar between Central and TE and between Eastern and TE. However, allopatric divergence is only rejected Central↔TE, not Eastern↔TE (see Supporting information, Table S5), and estimated gene flow rates are highest Central↔TE (Fig. 7), in support of the species tree topology.

DISCUSSION

Geographical patterns of divergence within *S. lateralis*

In the present study, we have analyzed multilocus sequence data using a combination of phylogenetic, cluster-based, and migration–divergence approaches to elucidate the evolutionary history that has shaped natural populations still engaged in the process of divergence. By accounting for the effects of gene flow and genetic drift on population history, we are able to make stronger inferences about relationships among lineages and assess the robustness of these inferences to ongoing gene flow. Sequence data best support three major lineages comprising seven populations that are distributed longitudinally across the species range. Inferred relationships among these populations are well-supported, regardless of whether or not samples most likely impacted by recent gene flow are included in the analysis.

The inferred tree is significantly more likely than one where group Western is constrained to be basal. Thus, the most likely geographical origin of extant *S. lateralis* diversity is in the extreme south-east region around Florida and Georgia. This is inferred despite the fact that the Texas populations are the

most genetically distinct and closest to completing the lineage sorting process (see haplotype and individual networks in the Supporting information, Figs S3, S4). Western is the first group to be distinguished from the rest of the species using hierarchical STRUCTURE analysis (i.e. at $K = 2$) and species tree analysis consistently supports an alliance between western populations when as few as two samples are randomly drawn from the dataset (whereas other nodes require at least 16 samples). Also, a basal group in Texas might have been expected if *S. lateralis* resulted from a northward expansion from Mexico, where its three New World congeners are currently distributed. New World *Scincella* are assumed to have resulted from a single dispersal event across the Bering Land Bridge during the Miocene (Honda *et al*., 2003; Macey *et al*., 2006). Although the biogeographical history of the group since its arrival is difficult to infer without additional sampling within the genus, these results do suggest that, if *S. lateralis* did expand from a southern ancestral population, diversification observed in extant populations did not commence until after the species reached the east coast. Basal lineages located in or around Florida have been reported for several other south-eastern taxa (Burbrink *et al*., 2008; Fontanella *et al*., 2008; Makowsky *et al*., 2010; Kubatko, Gibbs & Bloomquist, 2011), which is consistent with this region being an important refugium for vertebrates throughout the Pliocene and Pleistocene (Platt & Schwartz, 1990; Jackson *et al*., 2000). The general east to west direction of migration and the high estimates of genetic diversity in the east inferred using IM analysis (N_e estimates average three to five times larger for eastern relative to western populations) also support a scenario where western populations are ultimately derived from eastern migrants.

The heightened divergence in central Texas may partly be a result of western populations being geographically peripheral (Gavrilets, Li & Vose, 2000) and relatively isolated from the rest of the species. In central Texas, *S. lateralis* appears to be more patchily distributed, restricted to islands of mesic forest along major rivers (N. Jackson, pers. obs.). This could allow for the development of unique variation that fails to be shared with the rest of the species. This hypothesis is supported by a lack of STRUCTURE-inferred hybrid individuals between populations CTE and MW and in low estimates of migration CTE→MW. Enhanced isolation in combination with small population size (particularly estimated for CTW) could help explain the increased lineage sorting observed for the western group (see Supporting information, Fig. S3). This highlights the importance of accounting for population-level processes which result in stochastic Wright–Fisher sampling when estimating species' histories in recently divergent groups.

A species tree where population TE is nested within the central group is significantly more likely than one where TE is constrained to the eastern group. This relationship is also supported by mtDNA phylogeny (Jackson & Austin, 2010) and by long-term estimates of gene flow derived from IM analysis which are higher Central↔TE relative to Eastern↔TE. However, given that the species tree model does not distinguish shared alleles due to dispersal from those resulting from common ancestry, this heightened gene flow between TE and the central populations could mask the true evolutionary relationships among these groups. This possibility is exemplified by results from *BEAST analysis of datasets simulated under an alternative scenario in which TE diverged most recently from Eastern and subsequently shared migrants with Central. This led to well-supported inference of the incorrect branching pattern, showing that empirical estimates of migration inferred between TE and the central populations are sufficient to mislead species tree analysis. Thus, although gene flow appears to currently be greatest Central↔TE, it is unclear whether this gene flow reflects or obscures the true history of divergence. Additionally, it may be that a bifurcating model will fail to reflect the true nature of the relationship of TE in respect to eastern and central lineages. The Tombigbee River, which flows south through western Alabama into the Gulf of Mexico, has been an historically important isolating barrier for many taxa (Soltis *et al*., 2006; Pyron & Burbrink, 2009; Kubatko, Gibbs & Bloomquist, 2011) and may have played a role in the divergence between central and eastern groups. However, the geographical distribution of population TE inferred using STRUCTURE suggests that, although this river appears to approximately delineate TE and eastern populations when sampled near the Gulf Coast, it does not do so further north (Fig. 1), indicating that this river is not currently an important dispersal barrier north of the gulf. Alternatively, the Alabama River, although less often implicated in causing phylogeographical patterns, better predicts eastern–central population boundaries and thus may pose a greater isolating force in *S. lateralis* (Newman & Rissler, 2011). Regardless of the divergence history of these populations, TE currently shares ancestry with both eastern and central lineages in a way that may not be best captured by a tree. Similar divergence times estimated between Central and TE and Eastern and TE support this (Fig. 7).

Incomplete isolation of *S. lateralis* populations is also apparent in response to two other well-known dispersal barriers in the south-east: the Apalachicola and Mississippi Rivers. The Apalachicola River well defines the break between FP and EC populations in the Florida panhandle, although population EC is

found on both sides of the river in Georgia, suggesting that this river may not be as isolating as it once was north of the Gulf. These multilocus data differ from mtDNA in that they reflect a weaker barrier effect of the Mississippi River. Although the river divides two of the major mtDNA clades (approximately 6% uncorrected divergence), it does not delineate any of the three major nDNA-based groupings and only approximately delineates the two least divergent populations. Both datasets show a large region of population overlap across the Mississippi River in south-eastern Louisiana, likely resulting from frequent channel switching of the Lower Mississippi River.

The role of migration in divergence

A simple allopatric scenario was rejected for most population pairs evaluated, suggesting that ongoing gene flow occurs among populations. It is, however, notoriously difficult to determine whether inferred gene flow between populations is a result of migration occurring throughout the divergence process or to migration that has commenced recently upon secondary contact (Becquet & Przeworski, 2009; Strasburg & Rieseberg, 2011). In the case of parapatrically distributed populations, insight into the timing of migration may be attained by investigating variation in the geography of gene flow. When parapatric samples were removed from the dataset, we inferred lower estimates of gene flow and a reduced incidence of allopatric model rejection. Reduction in ability to reject allopatry is not likely explained by reduced statistical power in culled datasets given that widths of highest posterior density intervals do not significantly differ between culled and full analyses (paired t-test $P = 0.14$). Diminished gene flow in culled datasets suggests that a large amount of inferred gene flow between populations can be explained by contemporary introgression near population boundaries. This suggests that diversification has largely taken place in allopatry and that patterns of allele sharing among populations as a result of gene flow can be explained by recent relaxation of geographical dispersal barriers. This could have been facilitated by elevated barrier effects of rivers throughout the Pleistocene resulting from a combination of a restricted southern distribution of *S. lateralis* during glacial maxima (Capparella, 1991; Haffer, 1997) and also to widened basins and marine embayments characterizing peaks of deglaciation (Donoghue, 1989; Dowsett & Cronin, 1990). An exception to this may exist in the case of divergence between the central populations (MW and ME) and TE, where an IM model of divergence better fits the data. This sensitivity of inferred gene flow to geographical sampling highlights the importance of accounting for varying levels of migration across a species range when testing migration–divergence hypotheses (Leaché, 2009; Carling, Lovette & Brumfield, 2010). Datasets omitting sympatric/parapatric population samples may better reflect ancient estimates of gene flow between populations currently experiencing secondary contact.

Given that we have performed pairwise analyses, ignoring migration with 'ghost' populations, parameter estimates from IM analyses must be treated with caution (Beerli, 2004; Slatkin, 2005). However, our conclusion that individuals nearest the contemporary population boundaries have the highest impact on migration rate estimates should be robust because full and reduced datasets differ only in respect to their inclusion/exclusion of border samples. Additionally, parameter estimates obtained using the culled datasets of the present study are likely less impacted by ignored migration with ghost populations given that migration estimates among populations are generally lower and not significant. These datasets are also more appropriate for inferring species histories given that species tree methods are currently unable to account for gene flow among groups. That the same tree is inferred when samples most likely engaged in gene flow are removed from the dataset suggests that the inferred tree is generally robust to gene flow effects.

In addition to recent or long-term gene flow, more complicated migration–divergence scenarios are also plausible, although not distinguishable, using current methods. For example, simulations using a similar IM model suggest that if gene flow was present only during initial divergence but then ceased, allopatry may be incorrectly supported (Becquet & Przeworski, 2009). The effects of a cyclical recurrence of isolation and gene flow in response to fluctuating aridity throughout the Plio-Pleistocene would also be difficult to distinguish from a simpler IM model.

Origins of mtDNA and nDNA discordance

High mtDNA diversity and fragmentation have previously been observed in *S. lateralis*, with frequent isolation and divergence evident along the Gulf Coast resulting in 14 well-supported groups (see Supporting information, Fig. S1; Jackson & Austin, 2010). Here, in spite of additional sampling from divergent mtDNA haploclades, STRUCTURE best supports seven multilocus populations as found previously for nuclear (n)DNA (Jackson & Austin, 2010), indicating signal discordance between the two genomes.

Although the *BEAST topology is broadly consistent with a previously reconstructed mtDNA phylogeny, the depth and pervasiveness of divergence is greater in mtDNA relative to nDNA. Even after accounting for the four-fold difference in effective

population size between genomes, divergence times estimated here (between 90 000 and 505 000 years BP) are much more recent than estimates based on cyt *b* (which range from 1.3 to 7.4 million years BP when assuming a 1.5% divergence rate; Jackson & Austin, 2010), a discrepancy that cannot likely be explained by methodological differences underlying their estimation (Arbogast *et al*., 2002). Additionally, several geographically restricted mtDNA clades of significant divergence are wholly unrepresented in the nDNA, even though these clades exhibit similar levels of mtDNA divergence to those geographically larger clades that do have a nuclear counterpart (Jackson & Austin, 2010).

One plausible explanation for heightened mtDNA–nDNA discordance observed only in smaller coastal clades concerns the rate at which patterns of ancient divergence may be obscured by recent migration in nDNA versus mtDNA. If some populations along the Gulf Coast were isolated in small pockets of habitat at various times in the past (as a result of contraction of mesic habitat during arid cycles), subsequent secondary contact between these diverged groups may have disproportionately homogenized populations at nDNA, allowing uniparentally inherited mtDNA haplotypes to persist. This could have been aided by male-biased dispersal (Roca, Georgiadis & O'Brien, 2005; Yang & Kenagy, 2009). Although little is known about dispersal behavior in *S. lateralis*, estimates of home range are 3.6-fold higher for males than females (Brooks, 1967). Immigrants from neighbouring populations would have more readily overwhelmed built-up divergence in geographically smaller populations relative to larger ones given that the average distance of any individual to an adjacent population is reduced in the former relative to the latter. This possibility of differential loss of signal in the two genomes is supported by the observation that two cyt *b* haploclades separated by the Mississippi River in southern Louisiana largely remain isolated and distinct in the face of rampant mixed ancestry of nDNA-inferred populations ME and MW occupying this same region.

Simulations have shown that stochastic lineage sorting in combination with an isolation-by-distance pattern can produce deep phylogeographical breaks in nonrecombining DNA fragments, even when gene flow remains uninterrupted across the range of a population (Irwin, 2002; Kuo & Avise, 2005). In the absence of congruent fragmentation within independent loci, stochastic processes leading to observed geographically concordant mtDNA divergence cannot be ruled out, although it is unclear why this process would predominantly occur along the coast where population sizes are highest (Jackson & Austin, 2010) and where sampling is densest, given that these factors would be expected to reduce any stochastic effect (Irwin, 2002; Templeton, 2004). However, if populations near the coast were significantly smaller during evolutionary formative periods in the past (Jackson & Austin, 2010), this could have increased the plausibility of both stochastic mtDNA divergence and allopatric divergence followed by heightened gene flow for nDNA.

Summary

The inference of relationships among populations that have been shaped by a complex of processes such as gene flow, shifts in range and population size, extinction, and selection can be misled when relying on any one locus or phylogenetic approach (Rosenberg & Nordborg, 2002). Furthermore, genetic effects from these historical factors can be confounded with stochastic forces that also contribute to patterns of genetic variation (Wu, 1991; Arbogast *et al*., 2002; Hudson & Coyne, 2002). By analyzing multiple loci with a combination of species tree and migration–divergence population genetic analyses, we are able to make inferences about the divergence history within *S. lateralis* at the same time as accounting for population-level processes that lead to stochastic Wright–Fisher sampling, despite ongoing gene flow among groups. By investigating the geographical distribution of gene flow, we show that migration has occurred among divergent populations, although a significant amount of this gene flow can be attributed to recent migration. Excluding samples that are most likely to be engaged in contemporary gene flow may produce better estimates of parameters that govern historical divergence and help minimize impacts of gene flow when inferring phylogeny.

ACKNOWLEDGEMENTS

Special thanks are exteneded to R. Brumfield, B. Carstens, M. Hellberg, J. Oliver, and three anonymous reviewers for their helpful comments. Tissue loans were granted by L. Rissler (UA Herpetological Collection), R. Brown (KU), T. LaDuc (TNHC), C. J. Franklin (UTA), D. Dittman (LSUMZ), and J. Braun (OKMNH). Analyses were performed using High Performance Computing at Louisiana State University and the Computational Biology Service Unit at Cornell University. The present study was carried out under LSU IACUC protocol # 07–014 and funding was generously provided by the Louisiana Museum of Natural Science, Sigma Xi, LSU Biograds, and National Science Foundation grants DEB 0445213 and DBI 0400797 to C.C.A.

REFERENCES

Arbogast BS, Edwards SV, Wakeley J, Beerli P, Slowinski JB. 2002. Estimating divergence times from molecular data on phylogenetic and population genetic timescales. *Annual Review of Ecology and Systematics* **33:** 707–740.

Austin CC. 1995. Molecular and morphological evolution in South Pacific scincid lizards: morphological conservatism and phylogenetic relationships of *Papuan lipinia* (Scincidae). *Herpetologica* **51:** 291–300.

Austin CC, Spataro M, Peterson S, Jordon J, McVay JD. 2010. Conservation genetics of Boelen's python (*Morelia boeleni*) from New Guinea: reduced genetic diversity and divergence of captive and wild animals. *Conservation Genetics* **11:** 889–896.

Becquet C, Przeworski M. 2009. Learning about modes of speciation by computational approaches. *Evolution* **63:** 2547–2562.

Beerli P. 2004. Effect of unsampled populations on the estimation of population sizes and migration rates between sampled populations. *Molecular Ecology* **13:** 827–836.

Beerli P, Palczewski M. 2010. Unified framework to evaluate panmixia and migration direction among multiple sampling locations. *Genetics* **185:** 313–326.

Bohonak AJ. 2002. IBD (Isolation By Distance): a program for analyses of isolation by distance. *Journal of Heredity* **93:** 153–154.

Brooks GR. 1967. Population ecology of the ground skink, *Lygosoma laterale* (Say). *Ecological Monographs* **37:** 71–87.

Brown RP, Pestano J. 1998. Phylogeography of skinks (*Chalcides*) in the Canary Islands inferred from mitochondrial DNA sequences. *Molecular Ecology* **7:** 1183–1191.

Burbrink FT, Fontanella F, Pyron RA, Guiher TJ, Jimenez C. 2008. Phylogeography across a continent: the evolutionary and demographic history of the North American racer (Serpentes : Colubridae: *Coluber constrictor*). *Molecular Phylogenetics and Evolution* **47:** 274–288.

Capparella AP. 1991. *Neotropical avian diversity and riverine barriers. Acta XX Congressus Internationalis Ornithologici: New Zealand*. Wellington: *Ornithological Congress Trust Board*, 307–316.

Carling MD, Lovette IJ, Brumfield RT. 2010. Historical divergence and gene flow: coalescent analyses of mitochondrial, autosomal and sex-linked loci in *Passerina* buntings. *Evolution* **64:** 1762–1772.

Conant R, Collins JT. 1998. *Reptiles and amphibians of eastern and central North America, third ed*. New York, NY: Houghton Mifflin.

Coyne JA, Orr HA. 2004. *Speciation*. Sunderland, MA: Sinauer Associates.

Donoghue JF. 1989. Sedimentary environments of the inner continental shelf, northeastern Gulf of Mexico. *Gulf Coast Association of Geological Societies Transactions* **39:** 355–363.

Dowsett HJ, Cronin TM. 1990. High eustatic sea level during the middle Pliocene: evidence from the southeastern United States Atlantic Coastal Plain. *Geology* **18:** 435–438.

Drummond AJ, Rambaut A. 2007. BEAST: Bayesian evolutionary analysis by sampling trees. *BMC Evolutionary Biology* **7:** 214.

Eckert AJ, Carstens BC. 2008. Does gene flow destroy phylogenetic signal? The performance of three methods for estimating species phylogenies in the presence of gene flow. *Molecular Phylogenetics and Evolution* **49:** 832–842.

Edwards SV. 2009. Is a new and general theory of molecular systematics emerging? *Evolution* **63:** 1–19.

Evanno G, Regnaut S, Goudet J. 2005. Detecting the number of clusters of individuals using the software STRUCTURE: a simulation study. *Molecular Ecology* **14:** 2611–2620.

Falush D, Stephens M, Pritchard JK. 2003. Inference of population structure using multilocus genotype data: linked loci and correlated allele frequencies. *Genetics* **164:** 1567–1587.

Fetzner FWJ. 1999. Extracting high-quality DNA from shed reptile skins: a simplified method. *BioTechniques* **26:** 1052–1054.

Fontanella FM, Feldman CR, Siddall ME, Burbrink FT. 2008. Phylogeography of *Diadophis punctatus*: extensive lineage diversity and repeated patterns of historical demography in a trans-continental snake. *Molecular Phylogenetics and Evolution* **46:** 1049–1070.

Gavrilets S, Li H, Vose MD. 2000. Patterns of parapatric speciation. *Evolution* **54:** 1126–1134.

Haffer J. 1997. Alternative models of vertebrate speciation in Amazonia: an overview. *Biodiversity and Conservation* **6:** 451–476.

Harrigan RJ, Mazza ME, Sorenson MD. 2008. Computation vs. cloning: evaluation of two methods for haplotype determination. *Molecular Ecology Resources* **8:** 1239–1248.

Heled J, Drummond AJ. 2010. Bayesian inference of species trees from multilocus data. *Molecular Biology and Evolution* **27:** 570–580.

Hey J. 2010. Isolation with migration models for more than two populations. *Molecular Biology and Evolution* **27:** 905–920.

Honda M, Ota H, Kohler G, Ineich I, Chirio L, Chen SL, Hikida T. 2003. Phylogeny of the lizard subfamily Lygosominae (Reptilia : Scincidae), with special reference to the origin of the New World taxa. *Genes & Genetic Systems* **78:** 71–80.

Hudson RR, Coyne JA. 2002. Mathematical consequences of the genealogical species concept. *Evolution* **56:** 1557–1565.

Hudson RR, Kaplan NL. 1985. Statistical properties of the number of recombination events in the history of a sample of DNA sequences. *Genetics* **111:** 147–164.

Irwin DE. 2002. Phylogeographic breaks without geographic barriers to gene flow. *Evolution* **56:** 2383–2394.

Jackson ND, Austin CC. 2010. The combined effects of rivers and refugia generate extreme cryptic fragmentation within the common ground skink (*Scincella lateralis*). *Evolution* **64:** 409–428.

Jackson ST, Webb RS, Anderson KH, Overpeck JT, Webb T, Williams JW, Hansen BCS. 2000. Vegetation and environment in Eastern North America during the Last Glacial Maximum. *Quaternary Science Reviews* **19:** 489–508.

Johnson RM. 1953. A contribution on the life history of the lizard *Scincella laterale* (Say). *Tulane Studies in Zoology* **1:** 10–27.

Joly S, Bruneau A. 2006. Incorporating allelic variation for reconstructing the evolutionary history of organisms from multiple genes: an example from *Rosa* in north America. *Systematic Biology* **55:** 623–636.

Kass RE, Raftery AE. 1995. Bayes factors. *Journal of the American Statistical Association* **90:** 773–795.

Kubatko LS, Gibbs HL, Bloomquist EW. 2011. Inferring species-level phylogenies and taxonomic distinctiveness using multilocus data in *Sistrurus* rattlesnakes. *Systematic Biology* **60:** 393–409.

Kuo CH, Avise J. 2005. Phylogeographic breaks in low-dispersal species: the emergence of concordance across gene trees. *Genetica* **124:** 179–186.

Larkin MA, Blackshields G, Brown NP, Chenna R, McGettigan PA, McWilliam H, Valentin F, Wallace IM, Wilm A, Lopez R, Thompson JD, Gibson TJ, Higgins DG. 2007. Clustal W and Clustal X version 2.0. *Bioinformatics* **23:** 2947–2948.

Leaché AD. 2009. Species tree discordance traces to phylogeographic clade boundaries in North American fence lizards (*Sceloporus*). *Systematic Biology* **58:** 547–559.

Macey JR, Schulte JA, Strasburg JL, Brisson JA, Larson A, Ananjeva NB, Wang YZ, Parham JF, Papenfuss TJ. 2006. Assembly of the eastern North American herpetofauna: new evidence from lizards and frogs. *Biology Letters* **2:** 388–392.

Maddison WP. 1997. Gene trees in species trees. *Systematic Biology* **46:** 523–536.

Makowsky R, Marshall JC, McVay J, Chippindale PT, Rissler LJ. 2010. Phylogeographic analysis and environmental niche modeling of the plain-bellied watersnake (*Nerodia erythrogaster*) reveals low levels of genetic and ecological differentiation. *Molecular Phylogenetics and Evolution* **55:** 985–995.

Malhotra A, Thorpe RS. 2000. The dynamics of natural selection and vicariance in the Dominican anole: patterns of within-island molecular and morphological divergence. *Evolution* **54:** 245–258.

Milne I, Lindner D, Bayer M, Husmeier D, McGuire G, Marshall DF, Wright F. 2009. TOPALi v2: a rich graphical interface for evolutionary analyses of multiple alignments on HPC clusters and multi-core desktops. *Bioinformatics* **25:** 126–127.

Newman CE, Rissler LJ. 2011. Phylogeographic analyses of the southern leopard frog: the impact of geography and climate on the distribution of genetic lineages vs. subspecies. *Molecular Ecology* **20:** 5295–5312.

Nielsen R, Wakeley J. 2001. Distinguishing migration from isolation: a Markov chain Monte Carlo approach. *Genetics* **158:** 885–896.

Nylander JAA, Ronquist F, Huelsenbeck JP, Nieves-Aldrey JL. 2004. Bayesian phylogenetic analysis of combined data. *Systematic Biology* **53:** 47–67.

Platt WJ, Schwartz MW. 1990. Temperate hardwood forests. In: Randazzo AF, Jones DS, eds. *The geology of Florida*. Gainesville, FL: University Press of Florida.

Pluzhnikov A, Donnelly P. 1996. Optimal sequencing strategies for surveying molecular genetic diversity. *Genetics* **144:** 1247–1262.

Poulakakis N, Lymberakis P, Valakos E, Pafilis P, Zouros E, Mylonas M. 2005. Phylogeography of Balkan wall lizard (*Podarcis taurica*) and its relatives inferred from mitochondrial DNA sequences. *Molecular Ecology* **14:** 2433–2443.

Pritchard JK, Stephens M, Donnelly P. 2000. Inference of population structure using multilocus genotype data. *Genetics* **155:** 945–959.

Pyron RA, Burbrink FT. 2009. Lineage diversification in a widespread species: roles for niche divergence and conservatism in the common kingsnake, *Lampropeltis getula*. *Molecular Ecology* **18:** 3443–3457.

Roca AL, Georgiadis N, O'Brien SJ. 2005. Cytonuclear genomic dissociation in African elephant species. *Nature Genetics* **37:** 96–100.

Rosenberg NA, Nordborg M. 2002. Genealogical trees, coalescent theory and the analysis of genetic polymorphisms. *Nature Reviews Genetics* **3:** 380–390.

Slatkin M. 2005. Seeing ghosts: the effect of unsampled populations on migration rates estimated for sampled populations. *Molecular Ecology* **14:** 67–73.

Soltis DE, Morris AB, McLachlan JS, Manos PS, Soltis PS. 2006. Comparative phylogeography of unglaciated eastern North America. *Molecular Ecology* **15:** 4261–4293.

Stephens M, Scheet P. 2005. Accounting for decay of linkage disequilibrium in haplotype inference and missing data imputation. *American Journal of Human Genetics* **76:** 449–462.

Stephens M, Smith NJ, Donnelly P. 2001. A new statistical method for haplotype reconstruction from population data. *American Journal of Human Genetics* **68:** 978–989.

Strasburg JL, Rieseberg LH. 2010. How robust are 'isolation with migration' analyses to violations of the IM model? A simulation study. *Molecular Biology and Evolution* **27:** 297–310.

Strasburg JL, Rieseberg LH. 2011. Interpreting the estimated timing of migration events between hybridizing species. *Molecular Ecology* **20:** 2353–2366.

Suchard MA, Weiss RE, Sinsheimer JS. 2005. Models for estimating Bayes factors with applications to phylogeny and tests of monophyly. *Biometrics* **61:** 665–673.

Templeton AR. 2004. Statistical phylogeography: methods of evaluating and minimizing inference errors. *Molecular Ecology* **13:** 789–809.

Wakeley J, Hey J. 1998. Testing speciation models with DNA sequence data. In: DeSalle R, Schierwater R, eds. *Molecular approaches to ecology and evolution*. Basel: Birkhauser Verlag, 157–167.

Woerner AE, Cox MP, Hammer MF. 2007. Recombination-filtered genomic datasets by information maximization. *Bioinformatics* **23:** 1851–1853.

Wu CI. 1991. Inferences of species phylogeny in relation to segregation of ancient polymorphisms. *Genetics* **127:** 429–435.

Yang DS, Kenagy GJ. 2009. Nuclear and mitochondrial DNA reveal contrasting evolutionary processes in populations of deer mice (*Peromyscus maniculatus*). *Molecular Ecology* **18:** 5115–5125.

Zink RM. 2005. Natural selection on mitochondrial DNA in *Parus* and its relevance for phylogeographic studies. *Proceedings of the Royal Society of London Series B, Biological Sciences* **272:** 71–78.

SUPPORTING INFORMATION

Additional Supporting Information may be found in the online version of this article:

Figure S1. Approximate geographical distribution and relationships of 14 mitochondrial DNA clades based on cytochrome *b* haplotype data; reconstructed from Jackson and Austin (2010).

Figure S2. Population history parameters used to simulate divergence of Eastern, Central, and TE populations using SIMDIV. The simulation was repeated with and without migration between TE and Central populations. All parameter values were derived from isolation with migration (IM) analysis of the empirical dataset where parapatric samples are omitted. *mCentral→TE* was obtained by averaging *m* estimates between populations ME→TE and MW→TE. *mTE→Central* was obtained by averaging *m* estimates between populations TE→ME and TE→MW. θ*TE* is taken from the average θ estimate for TE across all relevant pairwise analyses and θ*East/TE* is obtained by averaging the estimated θ from the ancestral population from TE–FP and TE–EC pairwise analyses. The remaining simulated values of θ are taken from IM analyses performed using the entire dataset at once (i.e. where three populations were defined: 'Western', 'Eastern', and 'Central'. Otherwise, these analyses were carried out as explained in the text for the pairwise analyses). θ*Central* is the θ estimate for the Central population in an analysis where 'Central' = ME + MW (and where TE belongs to the Eastern group) and θ*East* is the θ estimate for the Eastern population in an analysis where 'Eastern' = FP + EC (and where TE belongs to the Central group). θ*East/TE/Central* is the estimate of θ from the ancestral population of Central (= ME + MW) and Eastern (= FP + EC + TE). Finally, in order to force the chronology of splitting times depicted above, *tEast-TE* comes from averaging splitting times (*t*) from ME – TE and MW – TE pairwise analyses and *tEast/TE-Central* is from the splitting time estimate between Central (= ME + MW + TE) and Eastern (= FP + EC) obtained from a three-population analysis.

Figure S3. Haplotype networks for eight loci used in the present study. Networks were estimated using TCS, version 1.21 (Clement *et al*., 2000) at the 95% confidence level. Circles represent unique haplotypes where the circle size is proportional to the number of samples per haplotype and circle fill colour is proportional to representation by each STRUCTURE population for a given haplotype. Lines connecting circles indicate mutations and black dots indicate inferred (but missing) haplotypes. Because reticulation was high for some loci as a result of recombination, to minimize difficulties in presenting reticulate histories we used the recombination-free dataset to estimate the networks shown. Doing this did not alter the overall structure of the networks; however, some singletons and mutations are therefore not represented. A few remaining network ambiguities (i.e. loops) were resolved according to rules laid out by Crandall and Templeton (1993) and Pfenninger & Posada (2002).

Figure S4. Phylogenetic networks constructed from multilocus data using the NeighborNet algorithm in SPLITSTREE, version 4.1. Tip shape and colour correspond to STRUCTURE populations. A, STRUCTURE-inferred hybrid samples are included (where hybrid individuals are highlighted with yellow rings. B, STRUCTURE-inferred hybrid samples are excluded. METHODS: To estimate multilocus distance-based networks, we first calculated pairwise uncorrected patristic distances (an analysis where corrected distances were used yielded a similar network). We then used POFAD, version 1.03 to convert this pairwise distance matrix of gene copies to a pairwise distance matrix of diploid individuals. To satisfy the assumption of a single independent history per locus, recombining segments were removed. Also, only samples for which there was no missing data (i.e. where all loci were present after removal of recombining sequences) were used. Networks were constructed using the NeighborNet algorithm (Bryant & Moulton, 2002) as implemented in SPLITSTREE, version 4.1 (Huson 1998; Huson & Bryant, 2006).

Table S1. List of samples used in the present study. GenBank accession numbers range from GQ450674–GQ451170 and JQ899454–JQ900088. L# = locality numbers. Asterisks denote missing sequence data.

Table S2. List of primers used in present study. All primers developed by Jackson & Austin (2010) except 5 (Townsend *et al*., 2008), and 6 (D. Leavitt, unpublished data).

Table S3. Diversity indices for all samples across eight loci (excluding outgroup). Bp, number of aligned basepairs; Alleles, number of alleles; VS, number of polymorphic sites; PSI, number of parsimony-informative sites; H_D, haplotype diversity; π, nucleotide diversity; *k*, mean number of pairwise differences; Max Div,

maximum uncorrected pairwise divergence. All calclulations were performed using DNASP, version 4.5 (Rozas *et al*., 2003) except for Max Div, which was calculated using MEGA, version 3.1 (Kumar, Tamura & Nei, 2004).

Table S4. Results from log-likelihood ratio (LLR) tests comparing full and nested models (a full isolation-with-migration model versus a strict allopatric model). A, tests were run for select pairwise analyses involving seven populations for full and reduced datasets (in which samples near parapatric boundaries were retained or removed, respectively). B, tests were performed for analyses involving Central (comprising ME and MW) and TE and Eastern (comprising FP and EC) and TE populations. Results highlighted in red indicate the analyses for which an allopatric model was rejected in a chi-squared test, given two degrees of freedom, after Bonferroni correction.

Table S5. Results from log-likelihood ratio (LLR) tests comparing full and nested models (a full isolation-with-migration model versus a strict allopatric model). A) Tests were run for select pairwise analyses involving seven populations for full and reduced datasets (wherein samples near parapatric boundaries were retained or removed, respectively). B) Tests were performed for analyses involving Central (comprising ME and MW) and TE and Eastern (comprising FP and EC) and TE populations. Results highlighted in red indicate analyses for which an allopatric model was rejected in a chi-square test, given two degrees of freedom, after a Bonferroni correction.